ING La Palma Technical Note no. 76

Wood's Anomalies in the INT spectrograph

Paul Murdin (RGO)

March 1990

Wood's anomalies in the INT spectrograph

1 Introduction

Fig 1 shows an IPCS observation of a standard star with the grating H2400B with the 235mm camera of the Intermediate Dispersion Spectrograph (IDS) of the Isaac Newton Telescope.

The corresponding spectrophotometric calibration of efficiency as a function of wavelength is in Fig 2.

The observation shows a curious spike at 3580A. The spike has been traced to a Wood's anomaly in the grating. This note draws attention to the existence of the phenomenon and its consequences for observing strategy.

2 Wood's anomalies

In 1902 R.W. Wood discovered that on many diffraction gratings narrow spectral regions showed sharp change of energy diffracted. Rayleigh explained these "anomalies" under the name "passing-off orders".

The physical explanation is the following.

Consider a reflection grating which produces a range of diffracted light in successive orders diffracted away from the normal. In some order, at some critical wavelength, the diffracted light lies in the plane of the grating. It is not possible for light beyond this point to be diffracted behind the glass of the grating. The power which would be sent into the forbidden region is redistributed back into the allowed orders ("passed off"). The power appears as an addition, to the spectrum response, with a sharp cut on at the critical wavelength and a steep decline to the red..

The additional power is in no sense a reflection or a ghost image. It is a genuine enhancement of efficiency of the grating, as if the light from two orders has been combined, which it has.

As can be imagined from the physical explanation, which involves light passing near the plane of the grating, the additional efficiency is highly polarisation-dependent - a Wood's anomaly is almost entirely polarised perpendicular to the grating rulings (the S-plane).

3 This observation

Fig 3 shows the geometry of the IDS and a grating,. The angle between the collimator axis and the camera axis is fixed mechanically at θ. $\theta = 35^o$ for the 235mm camera (and 25^o for the 500mm camera). The observed spectrum is near the camera-axis (at most, with the IPCS, 12.5 mm off axis at the 235 mm focal length, i.e. 3 degrees of deviation). The grating angle f3 defines the angle between the normal to the grating and the camera axis: it is near to the blaze angle, for the grating in the usual usage. The angle of incidence of light from the collimator is α, to the normal.

The grating equation is

$$\sin\alpha = m\lambda/2d + \sin\theta\ (2(1 + \cos\theta) - m^2\lambda^2/d^2)^{1/2}\ \ /\ \ 2(1 + \cos\ \theta)$$

where d is the groove separation (d = 0. 417 microns). In first order (m = 1) and with $\theta = 35^o$, we have at $\lambda = 0.37$ microns, $\alpha = 44.2^o$.

The anomalous wavelengths are given by

$$\lambda(W) = d\ (\sin \alpha \pm l\ )/n$$

where n = ± 1, ± 2, etc and the + sign in parenthesis is used when n is positive (and vice versa). For n = +2 we find

$$\lambda(W) = 0.357 \text{ microns}$$

This is closely what is observed. It is the near-coincidence of λ and $\lambda(W)$ which has made this anomaly observable in this case.

Fig 4 shows a calculation by I J Wilson , L C Botten and R C McPhedran (1976: "First, Second and Third Order Blazes of Diffraction Gratings" , University of Tasmania report DGRG 76/1) for the response of an infinite conductivity grating of blaze angle 10^{o} 22' and a range of Angles of Deviation (AD). The Wood's anomaly at $\lambda/d \sim 0.8$ seems to be the one detected.

4 Practical considerations

Since the responsivity is calibratable, in principle Wood's anomalies should not affect spectrophotometry. However, there are some caveats.

a) As Fig 4 dramatically illustrates, the grating response is highly dependent upon polarisation. Here, as elsewhere in spectrophotometry, observations of polarised sources are liable to error.

b) Again as Fig 4 demonstrates , the position of the Wood’s anomaly moves in wavelength as the grating angle is altered - it is obvious this must be so, since the position of the anomaly depends on the coincidence of the grating plane with a certain wavelength in a certain order. Obviously it is more important than usual to make calibration exposures under identical conditions to the programme exposures, i.e. don't move the grating.

c) As Fig 1 and Fig 4 show, Wood's anomalies are narrow in wavelength, in particular they have a very sharp cut-on. This means that spectrophotometric standards, observed with a spectral resolution comparable with the Wood's anomaly wavelength range cannot follow the response curve well. It would be necessary to use the standard star to fix the overall shape of the response curve and the original observation to determine its fine structure. Clearly the data in Fig 1 are not well enough observed to do this. Furthermore, the fitting of the curve in Fig 2 is not of high enough order even to fix the overall shape of the response curve.

d) Wood's anomalies in flat field exposures will be a nuisance.

The Wood's anomalies thus produce severe practical difficulties!

5 Wood's anomalies in other gratings

The equations of section 3 can be used to search for Wood's anomalies in other IDS gratings. Here is a list of examples found in the 235 camera in the IPCS wavelength range. In practice, the seriousness of these anomalies is unexplored (i.e. their amplitude). The fact that these Wood's anomalies have not been discovered in, e.g. flat fields, may mean that their amplitudes are insignificant (the UV anomaly which provoked this investigation would not have been found in a flat field exposure, under the usual circumstances). The vulnerable wavelength range is the range of central wavelengths which require a grating angle which produces a Wood's anomaly at a wavelength on the detector. The table shows an example calculation within the usual range of use of the gratings.

Grating	Vulnerable central wavelength range	Example(s) Central wavelength	Wood's anomalies (order n, and wavelength)	
2400	3000 - 4100	3500	+2	3520
1800	4100 - 5100	4500	+2	4680
1200	3600 - 4700	3800	-1	4000
1200	3600 - 4700	3800	+3	4222
1200	6300 -	6800	+2	6999
900	4500 - 6500	5500	-1	5134
900	4500 - 6500	5500	+3	5695
632	- 5200	5000	-2	4315
600	- 5300	5300	-2	4537
400	3700 -	4000	-3	5169
400	3700 -	5500	-3	4927
300	(all)	5500	-3	6865

Anomalies in the 500 mm camera are left as an exercise for the student.

6 Acknowledgments

I gratefully acknowledge the contributions of John Danziger of ESO, my co-observer, and the RGO Optics Group, Richard Bingham, Sue Worswick and David Jackson.

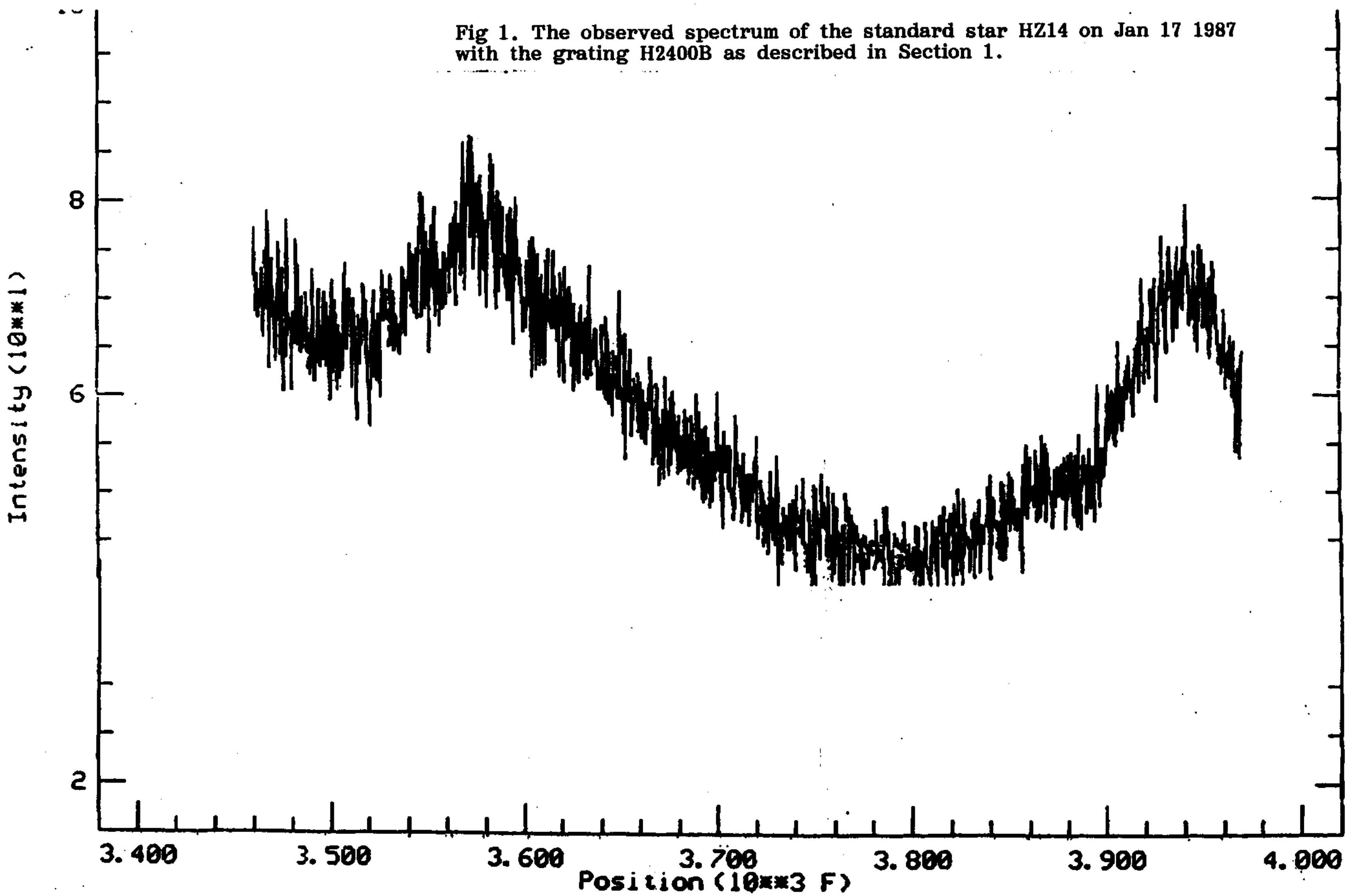

Fig 1. The observed spectrum of the standard star HZ14 on Jan 17 1987 with the grating H2400B as described in Section 1.

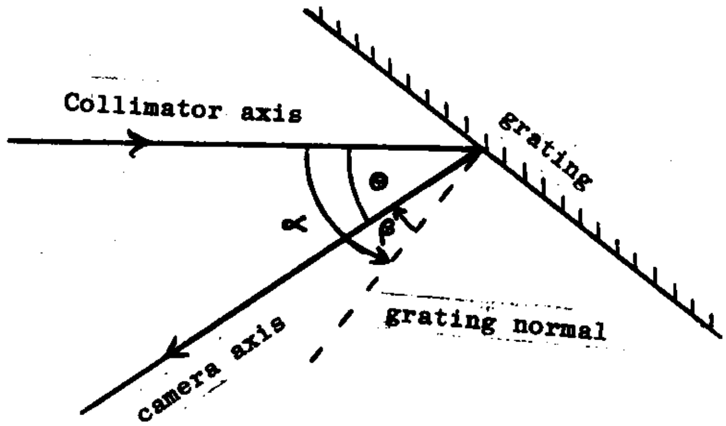

Figure 3 Geometry of the grating.

$\theta = 35^{o}$ for 235mm camera

$\theta = 25^{o}$ for 500mm camera

Figure 4 (next page) Calculated response curve by Wilson et al. (op. cit.) of the S and P polarisations for a grating with blaze angle 10^{o} 22’ at a range of three Angles of Deviation.

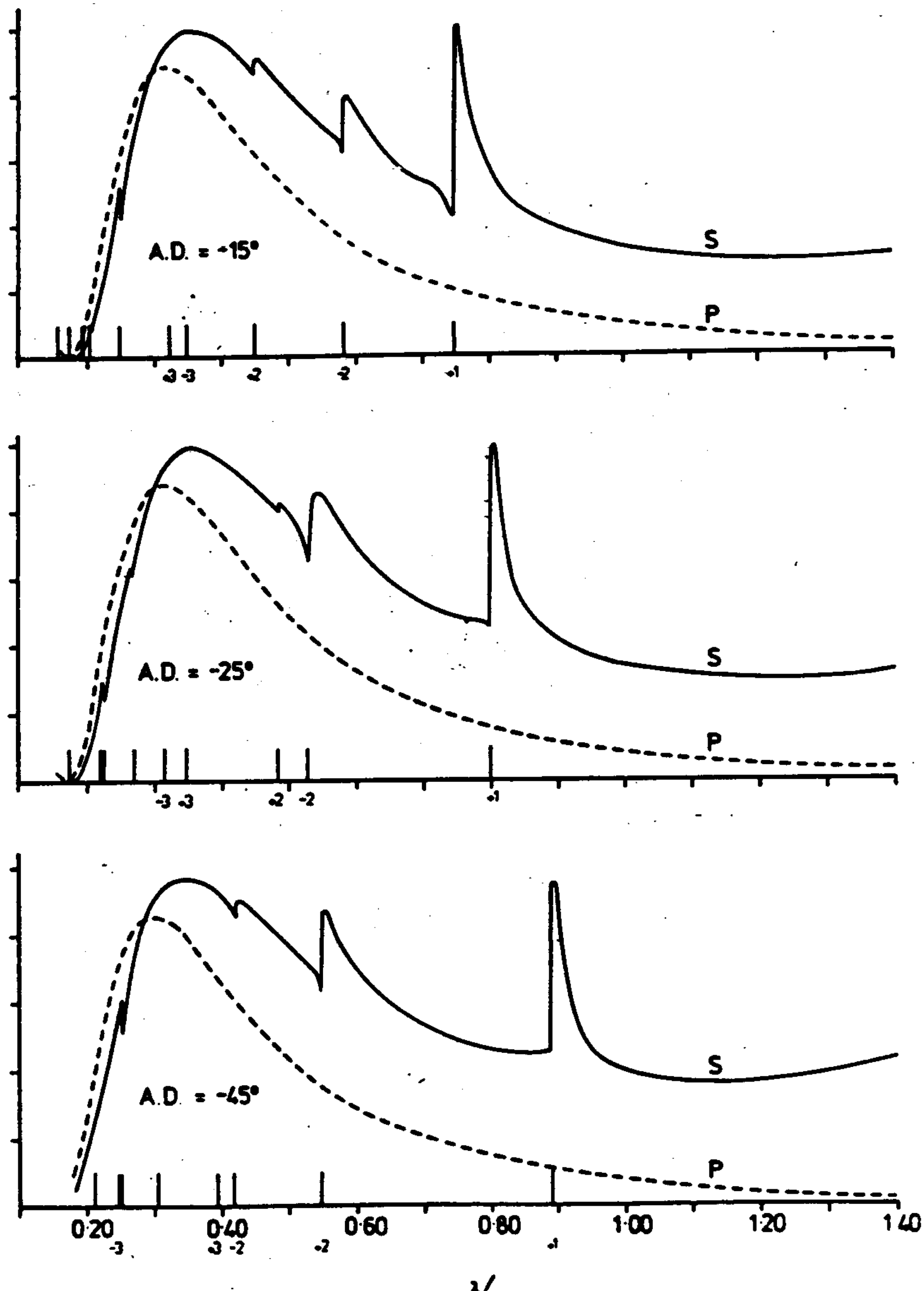

A.D. = -15°
S
P
-3 -3
-2
-2
-1
A.D. = -25°
S
P
-3 -3
-2 -2
-1
A.D. = -45°
S
P
0·20
0·40
0·60
0·80
1·00
1·20
1·40
-3
-3 -2
-2
-1
λ/d